Novel MEMS-IMU / Wi-Fi Integrated Indoor Pedestrian Location Algorithm

Minghong Zhu*, Ming Jin, Juan Liu, and Zhenpeng Wang

Abstract—**Indoor pedestrian location technology has been in focus because of the development in indoor positioning and navigation system. The focus is placed on how to reduce the time and economic costs by ensuring the positioning accuracy and positioning performance of the system. By utilizing Micro Electromechanical Systems - Inertial Measurement Unit (MEMS-IMU) in smart phones, this manuscript develops an integration strategy to directly estimate pedestrian location by combining MEMS-IMU and Wireless Fidelity (Wi-Fi) data. The work includes: 1) position estimation model relative to the reference coordinate system is established based on Pedestrian Dead Reckoning (PDR) algorithm; 2) gyroscope output in IMU is directly used as the original observation value, Wi-Fi positioning data is acquired at fixed frequency for system correction, and Extended Kalman Filter (EKF) algorithm is designed for estimating the real-time position coordinates of pedestrian; 3) the motion trajectory of pedestrians is designed, and algorithm efficacy and feasibility are verified by collecting the mobile phone sensors data and wireless signal Access Point (AP).**

Index Terms—**indoor pedestrian location, MEMS-IMU, Wi-Fi positioning, pedestrian dead reckoning.**

I. INTRODUCTION

IN modern cities, people's activity time in indoors accounts for about 80% of their living time. In mobile internet era, 70% of mobile phone-based dialog connection, mobile utilization, payment, data connection, 80% of internet data interaction, etc. occur in indoors [1]. Indoor positioning is thus widely used and required. Market value linked to indoor positioning and location services is on the rise [2]. The development of indoor pedestrian positioning and navigation technology can minimize self-positioning times for users and facilitate in users' activities and office work.

The primary objective of indoor pedestrian navigation and positioning technology is to reduce the system operating cost and improve the positioning accuracy. Smart phones are essential for the pedestrians of modern society to assist in their travels. Micro electromechanical systems—inertial measurement unit (MEMS-IMU) is embedded in smart phones to achieve completely autonomous inertial navigation and positioning [3], [4]. Compared with other navigation methods, the inertial navigation algorithm does not need external equipment, is not limited by external environmental conditions, and has greater degree of freedom for the movement. However, micro inertial measurement units (gyroscopes, accelerometers, magnetometers, etc.) have lower costs and reduced performance, and thus cannot be applied alone to the indoor pedestrian navigation. Therefore, when inertial navigation system based on MEMS-IMU works, fusion of information with other positioning technologies is required for attaining reliable positioning [5], [6]. The indoor environments are mostly equipped with wireless local area networks (WLAN) and wireless fidelity (Wi-Fi). Public places also provide free Wi-Fi hotspot access to the users. Wi-Fi positioning technology is presently the widely used indoor positioning algorithms, and navigation error does not accumulate with time. Wi-Fi positioning results can be combined with inertial navigation to correct the error of latter [7].

The optimal filter design improves integrated navigation accuracy and adoption of Kalman filter is widespread. Kalman filter based on integration mechanization adopts inertial navigation mechanization to estimate the error states and sensor systematic errors through aiding sensors measurements. Its strong dependence on *a-priori* inertial error model is bound to limit the use of low-cost inertial sensors (typically MEMS-IMU), because their time-variant noise model could be highly sensitive to the dynamic excitations and the temperature which are detrimental to the integrated system [8]. The system models used in Kalman filter are based on *a-priori* inertial error model, whether indirect or direct methods are adopted in conventional combination algorithm. IMU measurements are applied only in free inertial navigation calculation and no measurement updates are performed in Kalman filtering between the adjacent measurement epochs. In indoor navigation, Wi-Fi signal cannot provide position information during interruption or with inadequate signal. The drift of MEMS-IMU system error can lead to intolerable free inertial navigation solutions between the two auxiliary measurement updates. This manuscript proposes new indoor pedestrian location method by using IMU measurements in Kalman filter, especially for low-cost IMU. The method specifically, 1) establishes three-dimensional (3D) motion trajectory model based on pedestrian dead reckoning (PDR) as the key system model, so that the impact of time-variant errors of low-cost IMU on inertial navigation solution are alleviated; 2) establishes a measurement model based on output signal in the system (including gyroscope output in IMU) and distance obtained by Wi-Fi terminal (between wireless signal access point (AP) and mobile device), directly and independently participating in measurement updates of Kalman filtering, so that the dependence of inertial navi-

Manuscript received October 24, 2022; revised April 18, 2023. This work was supported in part by the National Natural Science Foundation of China under Grants 61871246 and 61971249; the Zhejiang Provincial Natural Science Funds for Distinguished Young Scholars under Grant LR21F010001; and the Ningbo Key Program of Natural Science Funds under Grant 202003N4013.

M. H. Zhu is a lecturer of Faculty of Electrical Engineering and Computer Science, Ningbo University, Ningbo 315211, P.R.China (corresponding author to provide e-mail: zhuminghong@nbu.edu.cn).

M. Jin is a professor of Faculty of Electrical Engineering and Computer Science, Ningbo University, Ningbo 315211, P.R.China (e-mail: jinming@nbu.edu.cn).

J. Liu is an associate professor of Faculty of Electrical Engineering and Computer Science, Ningbo University, Ningbo 315211, P.R.China (e-mail: liujuan1@nbu.edu.cn).

Z. P. Wang is a senior engineer of Sichuan Academy of Aerospace Technology, Chengdu 610100, P.R.China (e-mail: wzpdoctor@hrbeu.edu.cn).

gation mechanization on IMU measurements in traditional integration strategy is released; 3) independently models the systematic error of selected IMU measurement, so that the impact of IMU raw output noise can be reduced. This study uses raw outputs of inertial devices (angular velocity information of gyroscope) and combines distance information between AP point and mobile device measured via Wi-Fi signal strength. Navigation results are thus improved to provide stable and continuous indoor pedestrian navigation service location.

The manuscript structure is arranged as follows: firstly, 3D motion trajectory model based on PDR is established; secondly, a method for acquiring pedestrian position information based on Wi-Fi signal strength in specified reference coordinate system is discussed; thirdly, MEMS-IMU/Wi-Fi integrated indoor pedestrian location algorithm based on extended Kalman filter (EKF) is proposed; finally, pedestrian's indoor motion trajectory is designed, and the validity and feasibility of proposed localization algorithm are verified by collecting the data from mobile phone sensors and AP terminals.

II. Pedestrian motion model based on dead reckoning

The pedestrian motion model in this study consists of three parts considering human body as 3D rigid body: (1) location coordinate; (2) attitude angle; (3) angular velocity.

A. Location Model

The pedestrian dead reckoning (PDR) algorithm determines pedestrian current position by the position information at previous moment, movement distance between adjacent moments (or average speed in a time period) and heading information [9], [10]. Indoor positioning should first determine the reference coordinate system. If position coordinates under Earth Centered Earth Fixed (ECEF) frame are attained, they need conversion between geographical coordinate system (east-north-upright-handed, ENU) and ECEF frame. Considering that, 1) the location coordinate conversion will increase positioning error; 2) indoor positioning itself determines short-distance location information; and 3) indoor building signs can be confirmed and identified. Therefore, the reference coordinate system of position coordinates should be specified. This study selects body coordinate frame (b frame) at the initial position as reference coordinate system (B frame), and defines that the navigation coordinate frame (n frame) coincides with ECEF frame, as shown in Fig. 1

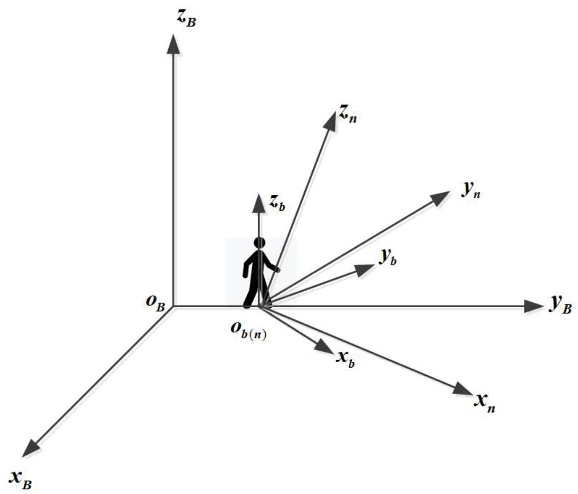

Fig. 1. Related coordinate systems in pedestrian navigation.

The proposed algorithm is suitable for calculating two-dimensional position information. The pedestrians current position information can be obtained by updating the horizontal position, if location environment is the same indoor floor, and ground is flat without obvious fluctuations. The slight height change in vertical direction may cause solution error in horizontal direction. The error can be compensated by corresponding step estimation model. The recursive formula of position coordinates based on the coordinate systems in Fig. 1 is established as follows:

Step 1: The estimated step length information is projected into n frame through heading angles. According to PDR algorithm, from epoch k to $k+1$, the pedestrians position increment in n frame is:

$$\Delta \mathbf{r}_{k+1}^{n} = \begin{bmatrix} \Delta E_{k+1} \\ \Delta N_{k+1} \end{bmatrix} = L_k \cdot \begin{bmatrix} \sin\psi_k \\ \cos\psi_k \end{bmatrix}, \tag{1}$$

where, ΔE_{k+1} and ΔN_{k+1} respectively represent the pedestrian position increment along East and north directions at epoch $k+1$. L_k is the estimated step length from epoch k to $k+1$. ψ_k is the heading estimation at epoch k. Combined with PDR algorithm, the principal diagram of above algorithm is as follows:

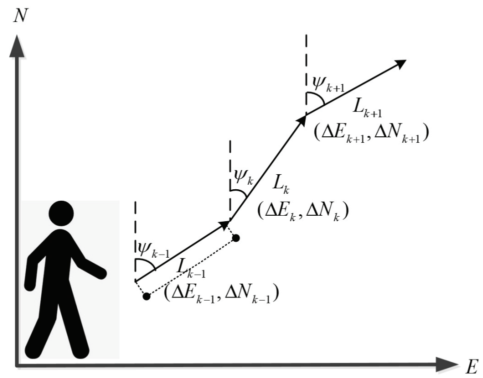

Fig. 2. Schematic diagram of pedestrian position increment calculation.

It is essential to first attain the one-step detection for acquisition of step length information. For each pedestrian step, the acceleration amplitude includes peak and trough values used for one-step detection. Specifically, through observing and comparing the vertical accelerometer output values for detecting amplitude changes (as shown in Fig. 3):

According to Weinberg's theory, pedestrian step length L_k during walking can be calculated from maximum and minimum values measured by vertical accelerometer:

$$L_k = \kappa \cdot (a_{\max}^{vert.} - a_{\min}^{vert.})_k^{\,1/4}, \tag{2}$$

where, $a_{\max}^{vert.}$ and $a_{\min}^{vert.}$ are the maximum and minimum values measured by vertical accelerometer respectively. κ is step estimation coefficient obtained through off-line training.

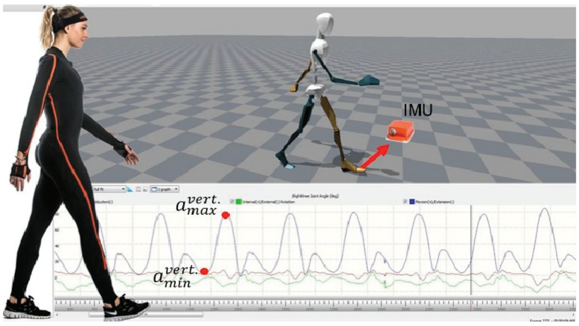

Fig. 3. Step detection using accelerometer output.

According to (1), the estimated heading ψ_k has role in PDR algorithm and is necessary to establish attitude recursive model.

Step 2: The pedestrian position vector relative to B frame at $k+1$ epoch is:

$$\mathbf{r}_{k+1} = \mathbf{r}_k + \mathbf{C}_t * \mathbf{C}_n^b * \Delta\mathbf{r}_{k+1}^n + \mathbf{w}_r, \tag{3}$$

where, $\mathbf{r} = \begin{pmatrix} x & y & z \end{pmatrix}^T$ is the position vector represented by triaxial coordinates in B frame; $\mathbf{w}_r$ is Gaussian white noise of position estimation vector; $\mathbf{C}_n^b$ is the directional cosine matrix from n frame to B frame; $\mathbf{C}_t$ is rotation matrix accumulated by the pedestrian relative to B frame. $\mathbf{C}_t$ is related to pedestrians heading changes, calculated as:

$$\mathbf{C}_t = \begin{pmatrix} \cos(\psi_0 - \psi_k) & \sin(\psi_0 - \psi_k) & 0 \\ -\sin(\psi_0 - \psi_k) & \cos(\psi_0 - \psi_k) & 0 \\ 0 & 0 & 1 \end{pmatrix}$$

where, ψ_0 is initial heading angle and ψ_k is heading angle at k epoch. It should be noted that ψ_k is the included angle between longitudinal axis projection of carrier on horizontal plane and north direction.

The pedestrians walking mode has unique characteristics. In most cases, pedestrians do not move laterally or vertically during indoor walking. This study thus adopts the idea of non-holonomic constraints (NHC) for pedestrian positioning, i.e., pedestrians position Δr_{k+1}^n relative to B frame in equation (1) is 2×1 dimension vector, however it is expanded to 3×1 dimension in equation (2) calculation. Herein, NHC idea utilization sets position increment on third line to zero, and takes only two-dimensional coordinates in oxy plane to calculate position coordinates.

B. Attitude Model

Euler angle of B frame relative to n frame (i.e., pitch, roll, and heading) is generally chosen to demonstrate rotation characteristics of 3D objects. The recursive formula of Euler angle can be realized by first-order Taylor series expansion:

$$\theta(k+1) = \theta(k) + \Delta t \mathbf{C}_{3\times3}\omega_{nb(k)}^b + \frac{\Delta t^2}{2}\mathbf{C}_{3\times3}\dot{\omega}_{nb}^b, \tag{4}$$

where,

$$\mathbf{C}_{3\times3} = \begin{pmatrix} \cos\gamma_{(k)} & 0 & \sin\gamma_{(k)} \\ \sin\gamma_{(k)}\tan p_{(k)} & 1 & -\cos\gamma_{(k)}\tan p_{(k)} \\ \sin\gamma_{(k)}\sec p_{(k)} & 0 & -\cos\gamma_{(k)}\sec p_{(k)} \end{pmatrix}$$

where, p, γ, ψ are pitch, roll and heading respectively. ω_{nb}^b is angular velocity in B frame, and $\omega_{nbx}^b, \omega_{nby}^b, \omega_{nbz}^b$ are ω_{nb}^b components in three axes. Angular acceleration $\dot{\omega}_{nb}^b$ is process noise of attitude vector, and $\mathbf{C}_{3\times3}$ is coefficient matrix of attitude model.

C. Angular Velocity Model

The angular rate is modeled as Gauss-Markov process for moving carrier. For pedestrians walking steadily in short time interval, the three components of angular velocity vector $\omega_{nb}^b = \begin{bmatrix} \omega_{nbx}^b & \omega_{nby}^b & \omega_{nbz}^b \end{bmatrix}^T$ in B frame are modeled as three independent random processes disturbed by random noise. ω_{nbx}^b and ω_{nby}^b are modeled as zero-mean random processes. ω_{nbz}^b is modeled as nonzero-mean random process. Assuming angular velocity as constant, the angular velocity vector at $k+1$ epoch is given as:

$$\begin{bmatrix} \omega_{nbx}^b \\ \omega_{nby}^b \\ \omega_{nbz}^b \end{bmatrix}_{k+1} = \begin{bmatrix} e^{-\frac{\Delta t}{T_x}}\omega_{nbx}^b \\ e^{-\frac{\Delta t}{T_y}}\omega_{nby}^b \\ e^{-\frac{\Delta t}{T_z}}\omega_{nbz}^b \end{bmatrix}_k + \begin{bmatrix} 0 \\ 0 \\ (1 - e^{-\frac{\Delta t}{T_z}}) \cdot \bar{\omega}_{nbz}^b \end{bmatrix} + \begin{bmatrix} w_{\omega_x} \\ w_{\omega_y} \\ w_{\omega_z} \end{bmatrix}, \tag{5}$$

where, Δt is time interval. T_x, T_y, T_z are the time correlation coefficients of first-order Markov model. $[w_{\omega_x}, w_{\omega_y}, w_{\omega_z}]^T$ are independent white noise of triaxial angular rate. $\bar{\omega}_{nbz}^b$ is nonzero-mean value of ω_{nbz}^b which can be replaced by angular velocity $\omega_{nbz(k-1)}^b$ of previous moment.

III. Algorithm Design of MEMS-IMU/Wi-Fi Integrated Indoor Pedestrian Location Filtering

Figure 4 depicts the schematic diagram of Wi-Fi/INS integrated navigation system of this study.

A. Measurement Vector

Firstly, the gyroscope output in IMU is selected as continuous observation. Gyroscope measurement is the angular velocity of b frame relative to inertial frame (i frame) in b frame and denoted by ω_{ib}^b. The measurement model ω_{ib}^b can be simplified as:

$$\omega_{ib}^b = (\mathbf{I} + \mathbf{S}_g)\omega_{nb}^b + \mathbf{b}_g + \mathbf{\Delta}_g, \tag{6}$$

where, $\mathbf{b}_g$ is gyroscope drift error including the initial value error and time-varying error; $\mathbf{S}_g$ is 3×3 dimension scale factor misalignment error matrix; and $\mathbf{\Delta}_g$ is the Gaussian white noise of gyroscope measurement vector.

Secondly, Wi-Fi information is collected at fixed frequency as auxiliary observation. According to Wi-Fi location principle, the real-time location information of pedestrians can be determined by AP location and the distance between AP and mobile device. Their relationship can be expressed by following equations:

$$\begin{cases} \sqrt{(x-x_1)^2 + (y-y_1)^2 + (z-z_1)^2} = d_1 \\ \sqrt{(x-x_2)^2 + (y-y_2)^2 + (z-z_2)^2} = d_2 \\ \sqrt{(x-x_3)^2 + (y-y_3)^2 + (z-z_3)^2} = d_3 \\ \cdots \\ \sqrt{(x-x_n)^2 + (y-y_n)^2 + (z-z_n)^2} = d_n \end{cases}, \tag{7}$$

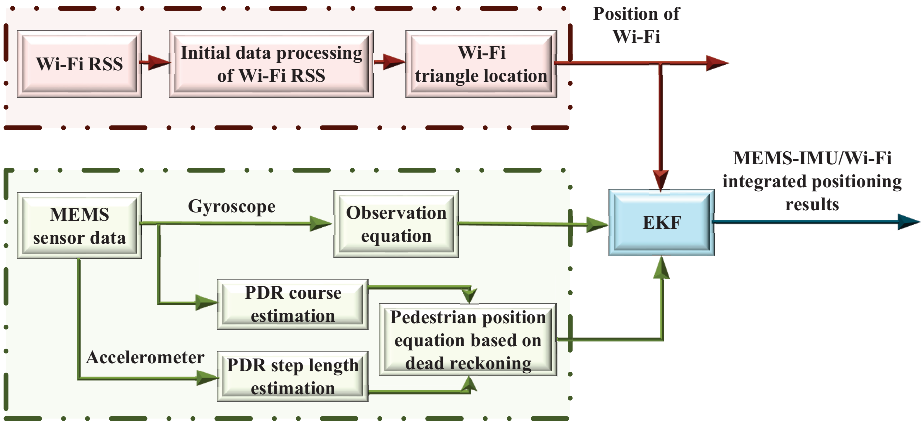

Fig. 4. Schematic diagram of Wi-Fi/INS integrated navigation system.

where, (x_n, y_n, z_n) is $n-$th AP position; (x, y, z) represents triaxial coordinates of position vector $\mathbf{r}$ and estimated for the mobile device; $d_i (i = 1, 2 \cdots n)$ is the distance between AP and mobile device as obtained from Wi-Fi signal strength through the following equation:

$$d = 10^{\frac{RSS+A}{-10n}}, \tag{8}$$

where, RSS is Wi-Fi signal strength received by the device through Wi-Fi receiving module in smart phone. A and n are propagation parameters and obtained through experiments on practical application environment. They are assumed as constants and solved from test data via the curve fitting technique.

B. State Vector

The state vector in this study is composed of two parts: the state describing pedestrian motion characteristics, and systematic error of gyroscope, as shown below (five 3×1 dimension vectors):

$$\mathbf{X}_{5\times1} = [\mathbf{r}^T \theta^T (\omega_{nb}^b)^T (\mathbf{b}_g)^T (\mathbf{s}_g)^T]$$

where, $\mathbf{r}$, θ and ω_{nb}^b are the position vector, attitude vector, and body angular velocity vector of pedestrians, respectively. $\mathbf{b}_g$ are $\mathbf{s}_g$ are the gyro drift and scale factor error, respectively. Under the assumption of high measurement noise level of MEMS-IMU, the systematic error vectors $(\mathbf{b}_g, \mathbf{s}_g)$ are independently modeled as random constant by using following equations:

$$\mathbf{b}_g(k+1) = \mathbf{b}_g(k) + \mathbf{w}_{b_g}, \tag{9}$$

$$\mathbf{s}_g(k+1) = \mathbf{s}_g(k) + \mathbf{w}_{s_g}, \tag{10}$$

where, $\mathbf{w}_{b_g}, \mathbf{w}_{s_g}$ are the white noise vectors.

C. Pedestrian Position Estimation Algorithm through EKF

Kalman filter algorithm is directly constructed based on the above state equations (3)-(5) and (9)-(10), and measurement equations (6)-(7). EKF linearization model at epoch k is described as:

$$\mathbf{X}_k = \mathbf{\Phi}_k \mathbf{X}_{k-1} + \mathbf{\Gamma}_k \mathbf{W}_k (Linearized\ system\ model), \tag{11}$$

$$\mathbf{Z}_k = \mathbf{H}_k \mathbf{X}_k + \mathbf{\Delta}_k (Linearized\ measurement\ model), \tag{12}$$

where, $\mathbf{X}_k$ is the n-dimensional state vector. $\mathbf{W}_k$ is m-dimensional process noise vector (as follows), and $\mathbf{W}_k \sim \mathrm{N}(0, \mathbf{Q}_k)$. $\mathbf{\Gamma}_k$ is coefficient matrix of $\mathbf{W}_k$. $\mathbf{Z}_k$ is p-dimensional measurement vector. $\mathbf{\Delta}_k$ is measurement noise vector, and $\mathbf{\Delta}_k \sim \mathrm{N}(0, \mathbf{R}_k)$. $\mathbf{\Phi}_k$ is state transition matrix. $\mathbf{H}_k$ is measurement matrix. $\mathbf{W}_k$ and $\mathbf{\Delta}_k$ are not interrelated.

$$\mathbf{W}_k = [(\mathbf{w}_r)^T, (\dot{\omega}_{nb}^b)^T, w_{\omega x}, w_{\omega y}, w_{\omega z}, (\mathbf{w}_{bg})^T, (\mathbf{w}_{sg})^T]^T$$

See Table 1 for the specific flow path of filtering algorithm.

TABLE I
SOLUTION OF KALMAN FILTER

One-step prediction of state vector and its variance matrix $\hat{\mathbf{X}}_{k/k-1} = \mathbf{\Phi}_{k-1} \hat{\mathbf{X}}_{k-1}$ $\mathbf{P}_{k/k-1} = \mathbf{\Phi}_{k-1} \mathbf{P}_{k-1} \mathbf{\Phi}_{k-1}^T + \mathbf{\Gamma}_{k-1} \mathbf{Q}_{k-1} \mathbf{\Gamma}_{k-1}^T$
Optimal estimation of state vector and its variance matrix $\hat{\mathbf{X}}_k = \hat{\mathbf{X}}_{k/k-1} + \mathbf{K}_k \mathbf{d}_k$ $\mathbf{P}_k = (\mathbf{I} - \mathbf{K}_k \mathbf{H}_k) \mathbf{P}_{k/k-1}$
System innovation and its variance matrix $\mathbf{d}_k = \mathbf{Z}_k - \mathbf{H}_k \hat{\mathbf{X}}_{k/k-1}$ $\mathbf{D}_{\mathbf{d}_k \mathbf{d}_k} = \mathbf{H}_k \mathbf{P}_{k/k-1} \mathbf{H}_k^T + \mathbf{R}_k$
Gain matrix $\mathbf{K}_k = \mathbf{P}_{k/k-1} \mathbf{H}_k^T \mathbf{D}_{\mathbf{d}_k \mathbf{d}_k}^{-1}$

IV. ROAD TEST AND RESULTS

Based on above theory and system model, this section designs set of experiments for verifying pedestrian location algorithm proposed in this study. Firstly, the walking path of one pedestrian is designed and real coordinates of real-time positions are recorded. Secondly, the data collector is devised to collect the data of triaxial accelerometers, gyroscopes, and magnetometers in IMU of pedestrian's smart phone. Thirdly, algorithm program is designed to process the collected sensor data for attaining the pedestrian position estimation. Finally, Wi-Fi signal is introduced to assist inertial sensor, and the position estimation results with or without Wi-Fi information are compared and analyzed.

A. Data Collection

An inertial navigation data collector is designed through Java programming to collect the data of triaxial accelerometers and gyroscopes, as shown in Fig. 5. The collected data is introduced into pedestrian position estimation algorithm program.

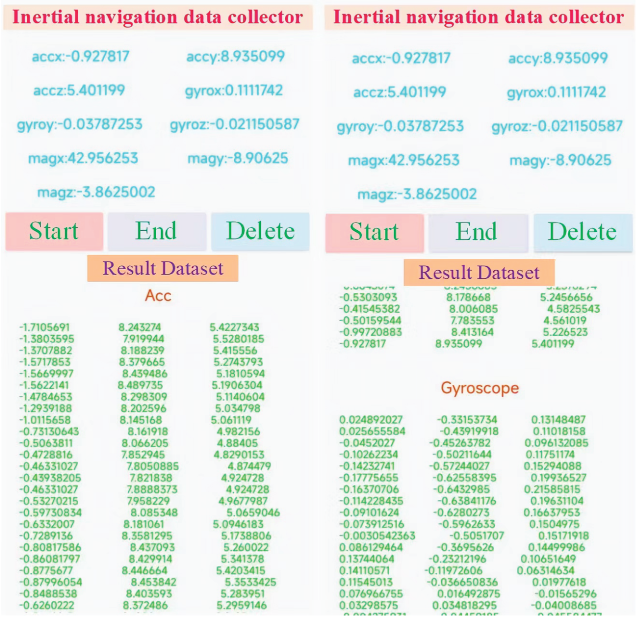

Fig. 5. Screen capture of inertial navigation data acquisition.

B. Wi-Fi Signal Collection

Mobile phone hotspot can be used as Wi-Fi signal to determine actual location of AP access point. Some signal acquisition information is shown in Fig. 6:

The device name is determined according to MAC address in Fig. 6. The distance d between each AP and pedestrian carrying the mobile device is inferred from signal strength, and distance value is directly used as observation value. After determining access frequency of observation data as per the number of data groups collected at different times, the distance d is embedded into pedestrian location algorithm for filtering and updating.

C. Measurement of Real Trajectory Data

Pedestrians need to design a walking path with smart phones to verify the algorithm accuracy. Experimental site is selected on the first floor of Ningbo University - Yang Youngman building, and trajectory adopts path of "straight line + right angle turn". The coordinates of real track as benchmark are obtained by counting the number of floor tiles as shown in Fig. 7. Difference between subsequent position estimation and this benchmark is the position estimation error.

D. Real Time Acquisition of Step Length

According to (2), the vertical acceleration information is used to calculate step length. Data collected by accelerometers is shown in Fig. 8:

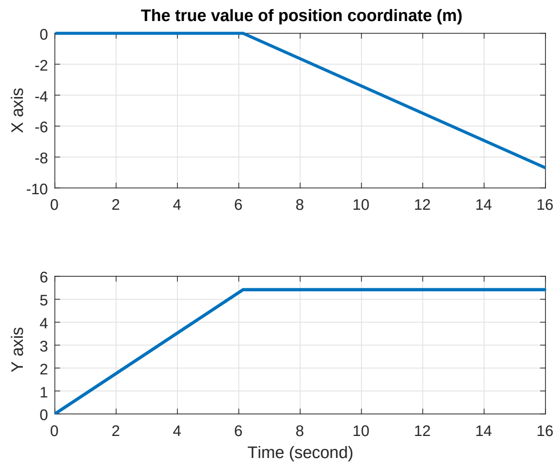

Fig. 7. Pedestrian real position coordinates.

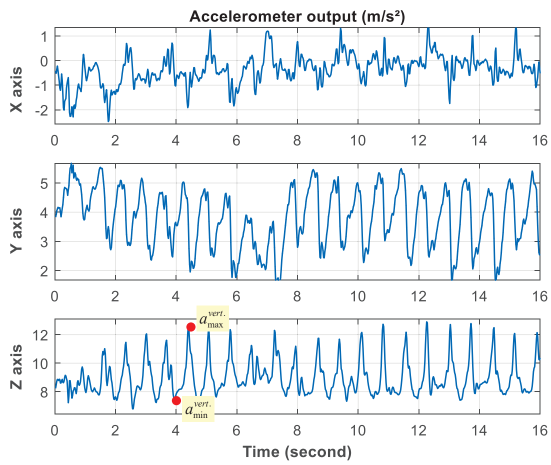

Fig. 8. Acceleration curve.

E. MEMS-IMU/Wi-Fi Integrated Indoor Pedestrian Location Results

Figure 9-11 reveal positioning results and error curves of this walking track calculated according to the built-in MEMS-IMU data of smartphone. Figure 12-15 depict the estimation results of MEMS-IMU/Wi-Fi integrated positioning.

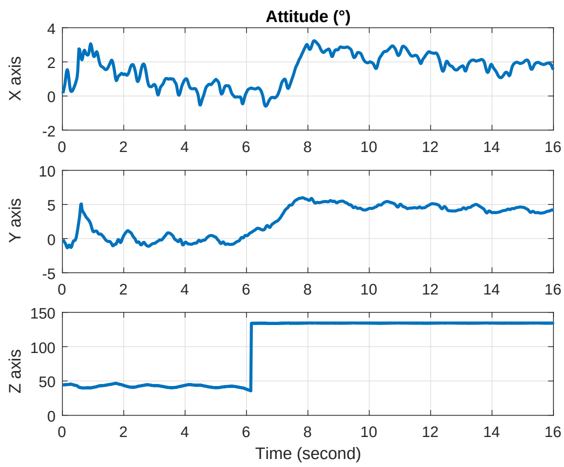

Fig. 9. Attitude estimation for MEMS-IMU positioning.

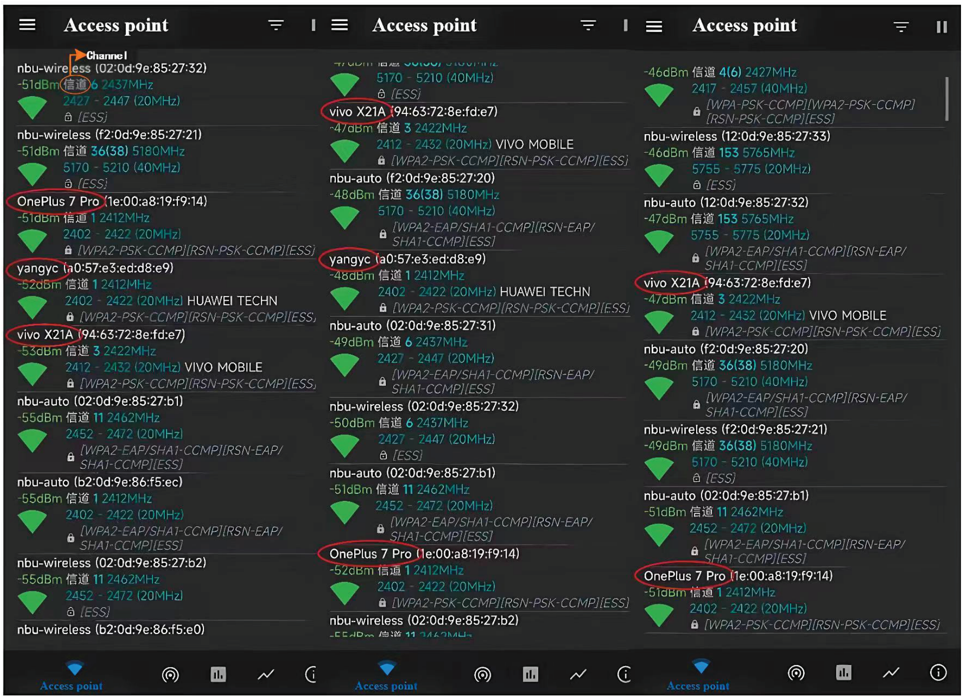

Fig. 6. Wi-Fi AP information.

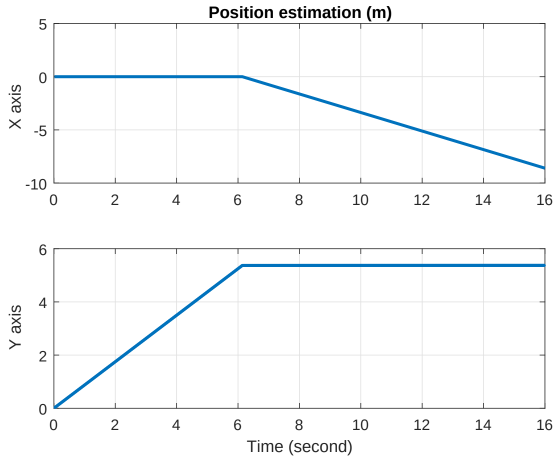

Fig. 10. Position estimation for MEMS-IMU positioning.

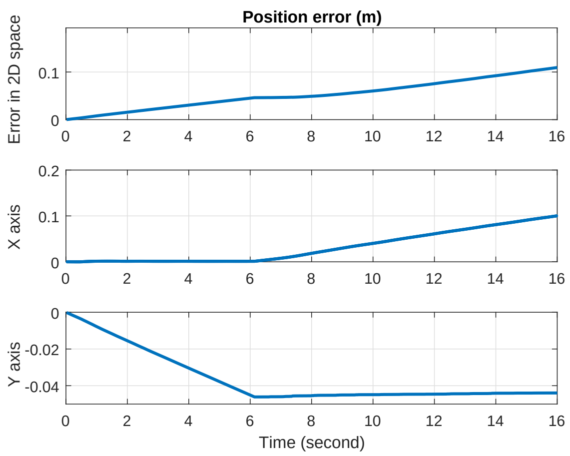

Fig. 11. Position error for MEMS-IMU positioning.

As shown in Figure 9-11, the positioning error using built-in IMU of smartphone slowly increases with time and reaches $0.1m$ during $16s$-walk (total walking distance of about $10m$). This is an effective positioning scheme as its error is within permissible limits.

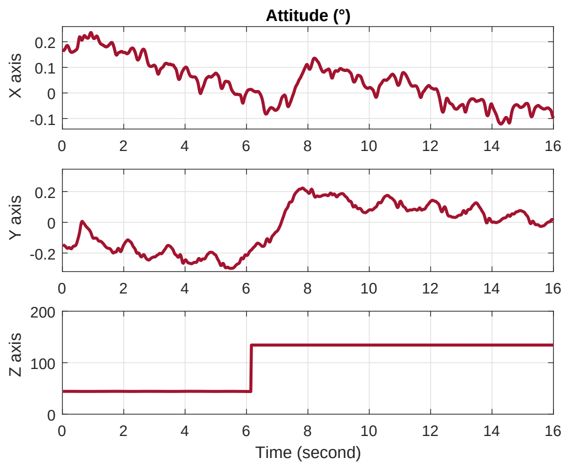

Fig. 12. Attitude estimation for MEMS-IMU/Wi-Fi integrated positioning.

There are 10 groups of Wi-Fi data collected at different times during $16s$-walk at access frequency of $0.625Hz$. Figure 12-14 exhibit the state estimations of MEMS-IMU/Wi-Fi integrated positioning, including attitude estimation, position estimation, and position error. As shown in Fig. 15, attitude estimation is more stable with Wi-Fi information assistance, which is also in accordance with pedestrian's attitude change under designed path (pitch and roll angles fluctuate slightly around zero; heading angle fluctuates less around initial value and increases by about 90° after right-angle turning). According to (3), attitude matrix is the key to position coordinate transformation, and accuracy of attitude angle

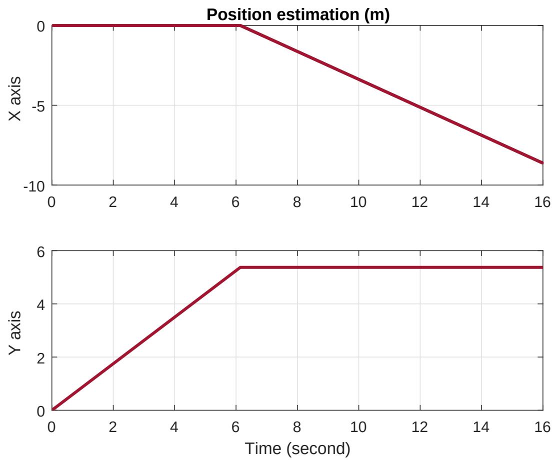

Fig. 13. Position estimation for MEMS-IMU/Wi-Fi integrated positioning.

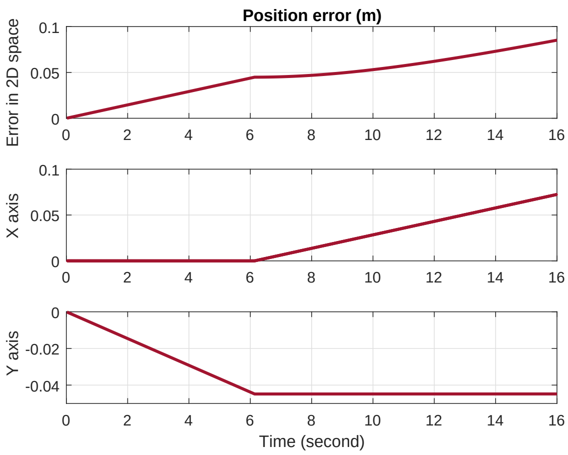

Fig. 14. Position error for MEMS-IMU/Wi-Fi integrated positioning.

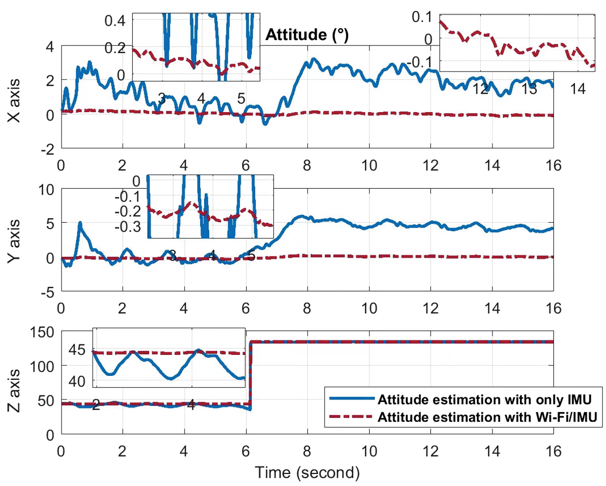

Fig. 15. Comparison of attitude estimation between two positioning methods.

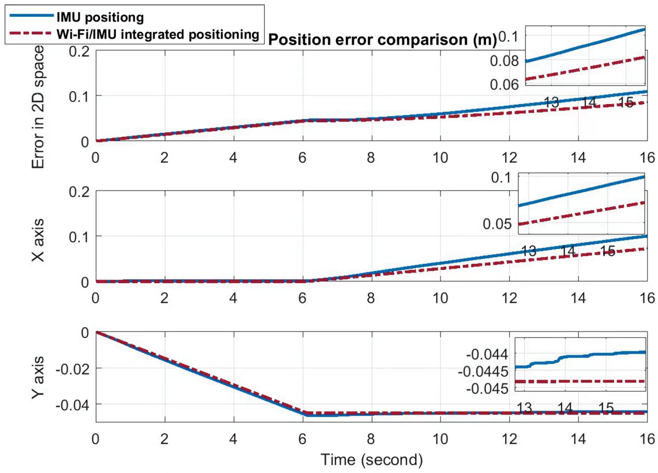

Fig. 16. Comparison of position error between two positioning methods.

estimation affects the position estimation accuracy. Figure 16 shows that during this process, the positioning error using built-in IMU slowly increases with time and exceeds $0.1m$, while in MEMS-IMU/Wi-Fi integrated positioning, error is within $0.1m$. Wi-Fi information can thus improve the pedestrian positioning accuracy.

V. Conclusion

The research on low-cost, high-performance, and real-time positioning technology has important strategic significance, particularly with the development of global information and intelligent industry. The problems such as serious drift of navigation solutions caused by time-varying errors of MEMS-IMU, require conducive integration of MEMS-IMU and other positioning technologies in indoor positioning system. This manuscript presents a novel indoor pedestrian navigation and positioning algorithm based on MEMS-IMU/Wi-Fi, which changes the working mode of conventional inertial sensor. This method achieves direct estimation of navigation parameters and IMU systematic errors through modeling. It makes system observations to directly and independently participate in KF measurement update. The proposed inertial sensor solution strategy is particularly applicable to MEMS-IMU. More reliable location information can be provided for pedestrians by combining output information of MEMS-IMU in smartphones and location data of indoor Wi-Fi. It is verified that the position error slowly increases with time when using built-in IMU, but within permissible range. The position error is reduced with MEMS-IMU/Wi-Fi integrated positioning as compared to IMU alone. Therefore, with the novel inertial sensor solution strategy, Wi-Fi assisted MEMS inertial sensor can accurately complete the indoor pedestrian navigation and positioning task. The algorithm proposed in this manuscript has certain efficacy and feasibility.

References

[1] Z. Wang, Z. Yang and Z. Wang, “An Adaptive Indoor Positioning Method Using Multisource Information Fusion Combing Wi-Fi/MM/PDR[J],” in *IEEE Sensors Journal*, vol. 22, no. 6, pp. 6010-6018, 2022.
[2] R. Mautz, “Indoor positioning technologies[D],” in *Zürich: Eidgenössische Technische Hochschule Zürich*, 2012.
[3] H. Zhao, W. Cheng, N. Yang, et al., “Smartphone-based 3D indoor pedestrian positioning through multi-modal data fusion[J],” in *Sensors*, vol. 19, no. 20, 4554, 2019.

[4] H. Xia, J. Zuo, S. Liu, et al., "Indoor localization on smartphones using built-in sensors and map constraints," *IEEE Transactions on Instrumentation and Measurement*, vol. 68, no. 4, pp. 1189-1198, 2018.
[5] C. Kou, H. Zhang and P. Wang, "Indoor positioning algorithm of pedestrian based on inertial sensor," *Transducer and Microsystem Technologies*, vol. 38, no. 1, pp. 137-140, 2019.
[6] N. Bai, Y. Tian, Y. Liu, et al.,"A high-precision and low-cost IMU-based indoor pedestrian positioning technique," *IEEE Sensors Journal*, vol. 20, no. 12, pp. 6716-6726, 2020.
[7] L. Huang, B. Yu, H. Li, et al.,"HPIPS: A high-precision indoor pedestrian positioning system fusing WiFi-RTT, MEMS, and map information," *Sensors*, vol. 20, no. 23, 6795, 2020.
[8] M. Zhu, F. Yu, S. Xiao, et al., "An improved posteriori variance-covariance components estimation applied to unconventional GPS and multiple low-cost imus integration strategy," *IEEE Access*, vol. 7, no. 1, pp. 136892-136906, 2019.
[9] P. Deng, F. Zhu and R. Zhao, "An indoor inertial navigation and positioning algorithm based on accurate heading angle correction," *Journal of Chinese Inertial Technology*, vol. 28, no. 6, pp. 716-722, 2020.
[10] X. Tao, T. Shi, X. Ma, et al., "An improved indoor pedestrian dead reckoning algorithm using ambient light and sensors," *Multimedia Tools and Applications*, vol. 81, pp. 32581-32592, 2022.